minerals

MDPI

Article

Effectiveness of Fly Ash and Red Mud as Strategies for Sustainable Acid Mine Drainage Management

Viktoria Keller [1], Srećko Stopić [1,*], Buhle Xakalashe [2], Yiqian Ma [1], Sehliselo Ndlovu [3], Brian Mwewa [3], Geoffrey S. Simate [3] and Bernd Friedrich [1]

1 IME Process Metallurgy and Metal Recycling, RWTH Aachen University, 52056 Aachen, Germany; viktoria.keller@rwth-aachen.de (V.K.); yma@ime-aachen.de (Y.M.); bfriedrich@ime-aachen.de (B.F.)
2 Pyrometallurgy Division, MINTEK, Private Bag X3015, Randburg 2125, South Africa; buhlex@mintek.co.za
3 School of Chemical and Metallurgical Engineering, University of the Witwatersrand, Johannesburg 2000, South Africa; Sehliselo.Ndlovu@wits.ac.za (S.N.); sirbhimself@yahoo.co.uk (B.M.); Geoffrey.Simate@wits.ac.za (G.S.S.)
* Correspondence: sstopic@ime-aachen.de; Tel.: +49-176-7826-1674

Received: 7 June 2020; Accepted: 6 August 2020; Published: 10 August 2020

Abstract: Acid mine drainage (AMD), red mud (RM) and coal fly ash (CFA) are potential high environmental pollution problems due to their acidity, toxic metals and sulphate contents. Treatment of acidic mine water requires the generation of enough alkalinity to neutralize the excess acidity. Therefore, red mud types from Germany and Greece were chosen for the neutralization of AMD from South Africa, where this problem is notorious. Because of the high alkalinity, German red mud is the most promising precipitation agent achieving the highest pH-values. CFA is less efficient for a neutralization and precipitation process. An increase in temperature increases the adsorption kinetics. The maximum pH-value of 6.0 can be reached by the addition of 100 g German red mud at 20 °C to AMD-water with an initial pH value of 1.9. German red mud removes 99% of the aluminium as aluminium hydroxide at pH 5.0. The rare earth elements (yttrium and cerium) are adsorbed by Greek red mud with an efficiency of 50% and 80% at 60 °C in 5 min, respectively.

Keywords: acid mine drainage; secondary materials; management; absorption; precipitation

1. Introduction

AMD is a term for wastewaters from mining processes. AMD contains a high concentration of dissolved metals from ores in a sulphate solution [1,2]. While mining, the mass of the rocks is fragmented. This leads to an increase of the surface area contacting the atmosphere which results in higher acid production rate [3]. As mentioned by Tabelin et al. [4] the contaminated excavation debris/spoils/mucks, loosely referred to as "naturally contaminated rocks", contain various hazardous and toxic inorganic elements like arsenic (As), selenium (Se), boron (B), and heavy metals like lead (Pb), cadmium (Cd), copper (Cu), and zinc (Zn). If left untreated, these naturally contaminated rocks could pose very serious problems not only to the surrounding ecosystem but also to people living around the construction and disposal sites.

Park et al. [5] mentioned that remediation options like neutralization, adsorption, ion exchange, membrane technology, biological mediation, and electrochemical approach have been developed to reduce the negative environmental impacts of AMD on ecological systems and human health. However, these techniques require a continuous supply of chemicals and energy, expensive maintenance and labor cost, and long-term monitoring of affected ecosystems until AMD generation stops.

As mentioned by Igarashi et al. [6], AMD containing Zn, Cu and As was treated by using a laboratory-type continuous ferrite process flow setup. Cu and As were removed in the first sludge,

which are stable in standard leaching tests. Magnetic magnesioferrites and magnetite were generated when dissolved silicon (Si) was low. However, in the study by Igarashi et al., information about the recovery of critical metals such as rare earth elements is missing.

AMD also originates from sulphide conglomerates stored on deposits where the rain rinses the acid and metals such as uranium (U) out of the dumps [3]. Finally, the acid infiltrates the groundwater and the environment such as rivers in the affected region around the deposits which contaminates the aquatic life and the soil in the surroundings [7]. Additionally, South Africa is a water-poor country with an average rainfall of under 450 mm per year [7]. Acid mine drainage containing around 3500 mg/L [3] of sulphate has a pH value between 2 and 3 which increases the solubility of certain metals such as heavy metals. Along the river pathways, the iron (Fe) in a sulphide form oxidizes and precipitates, leading to a bright orange trail. The formation of AMD is the result of oxidation of pyrite, FeS_2, with oxygen and ferric iron, Fe^{3+}, as shown in Equations (1)–(3) [8]. Consequently, sulphuric acid is formed during this reaction. At this pH, bacteria like *Thiobacillus ferrooxidans* can survive [7] and accelerate the geochemical reactions.

$$FeS_{2(s)} + \frac{7}{2}O_{2(aq)} + H_2O \rightarrow Fe^{2+} + 2{SO_4}^{2-} + 2H^+ \quad (1)$$

$$Fe^{2+} + \frac{1}{4}O_{2(aq)} + H^+ \rightarrow Fe^{3+} + \frac{1}{2}H_2O \quad (2)$$

$$Fe^{3+} + 3H_2O \rightarrow Fe^{3+} + 3OH^- + 3H^+ \rightarrow Fe(OH)_{3(s)} + 3H^+ \quad (3)$$

AMD can be classified by the content of acid and dissolved metals with Ficklin diagram [9]. At the surface, the AMD stream is diluted by rain or surface water which leads to an increase of the pH values with white precipitation products in the AMD stream. The precipitation products contain mainly crystalline and amorphous aluminium phases [10] which adsorb other metals. Heavy metals are generally removed by iron precipitation. Aluminum precipitation only becomes important when iron content is low, but this is rarely the case.

In South Africa, coal is extracted by underground mining or open-pit mining with little surface dumping [3]. FeS_2 is contained in the host rock but is more abundant in the coal layers. When mining terminates, the mine will be closed by collapsing the upper layers. Water fills in the voids of the fractured rocks and reacts with the FeS_2 [3]. Rain penetrates through the soil and becomes acidic and influences the natural groundwater. In the dams around coal mines in Middelburg and Witbank in South Africa, the salinity and sulphate concentration amount to about 200 mg/L [3], which is the limit for domestic use.

Regarding the problem of growing deposits, the branch of research on wastewater treatment is of high importance. The primary aim of wastewater treatment is to recover valuable metals and neutralize the acidic solution [11]. An advantage is the higher content of valuable metals in the wastewater compared to the ores used in primary production.

There are further possibilities for water purification like the SAVMIN™ process. This is the simplest technology for reducing high sulphate concentrations is lime precipitation developed by MINTEK in South Africa [9]. Precipitation of metal hydroxides and sulphides was performed using sodium hydroxide, calcium carbonate and hydrogen sulphide. Regarding the costs, calcium carbonate is most suitable for the neutralization experiments. Because the neutralization is exothermic, room temperature was chosen for the removal of metals from waste solution. Pre-oxidation with hydrogen peroxide transforms the bivalent Fe to the trivalent Fe which precipitates at lower pH values [12] than the bivalent Fe. Analogously, As is oxidised from the trivalent state to the pentavalent state to enable hardly dissolving oxides [13,14]. Removal of As(III) and As(V) can occur during neutralization simultaneously. Additionally, because of the high reactivity of sulphides with heavy metal ions, they can be applied to achieve a larger decrease in metal concentration after neutralization with hydroxides [13]. Trivalent Fe cannot be removed by sulphides precipitation since they do not form stable sulphides under

wastewater conditions [13]. Instead, the trivalent will be reduced to the bivalent state which forms iron(II) sulphide (FeS) [14]. Another possibility for selective removal of metals is cementation with nanoscaled zerovalent powders which have a large reaction surface area [15]. Cementation at room temperature and reductive precipitation took a short time in contrast to adsorption. There is a tendency that metals are adsorbed in this sequence: Fe(II)/Fe(III) > Cu(II) > Mn(II) > Zn(II) [16] following the Langmuir model which states that all surfaces of a given solid have the same affinity to adsorb metals [17]. Addition of brine can decrease the kinetics of neutralization, so there is a long-term effect which avoids a too-high pH value [18]. Precipitation of dissolved metals is achieved by the introduction of chemical additives such as sodium carbonate and oxalic acid to mostly affect changes in pH and/or ligand concentration at room temperature.

High standards are applied for drinking water which is chosen as a better reference in comparison to the purified water. Pure water is clear, colour- and tasteless and low in microbiological contamination [14]. Some metals, like Fe^{3+}, change the colour of water. Fe^{3+} turns the water into a reddish-brown colour [19]. The optimum pH for drinking water ranges between 6.5–8.5 [19]. The taste threshold for salts depends on the cation (sodium, potassium) and the anion (chloride, sulphate) concentrations. For sodium chloride, the taste threshold concentration is 200–300 mg/L [19]. Turbidity indicates any kind of contamination which can be caused by inorganic and organic matter in the form of suspended particles [19]. Microorganisms are attached to particles [14]; therefore, filtration of particles can reduce their population in treated water. Turbidity of AMD can also be a sign of natural precipitation of iron. In Germany, the most important laws for wastewater treatment are:

- Water Resources Act (WHG, Wasserhaushaltsgesetz) [1]
- Wastewater Ordinance (AbwV, Abwasserverordnung) [20]
- Drinking Water Ordinance (TrinkwV, Trinkwasserverordnung) [21]

The European and German standards are based on the recommendations of the World Health Organization (WHO) [14], which has set up health-based guidelines for chemicals in drinking water [19]. The effects of contaminants on taste, odour and appearance are cited by the WHO, while the most important effects such as toxicity are not mentioned [19]. Mostly, because the concentration in treated water is too low, it is not possible to determine guideline values for some metals such as silver (Ag) and gold (Au). In the case of aluminium, the guideline value is nine-fold higher than the value achievable by current technology [19]. The TrinkwV restricts the concentration of aluminium since there could be a correlation between aluminium consumption and Alzheimer's diseases [14]. The pH value of drinking water is between 6.5 and 9.5. Water with carbonic acid (H_2CO_3) can have a lower pH value than 6.5 [21].

Purification of wastewaters is a high-complex process. The process line depends on the origin of the wastewater and therefore the contaminations as well as the subsequent use of the purified water. For use as drinking water, the water needs to fulfil special regulations, for example, the TrinkwV [21]. The purification process contains several steps such as mechanical separation of solids and suspended particles (e.g., flotation, sedimentation, filtering) [14,22]; oxidation of dissolved metals to solids [14]; ion exchange processes to neutralize the water from salts and metals [23]; disinfection of water by oxidation media (ClO_2, O_3, hyper chlorites) or UV-light [24] and biological treatment (aerobic processes and anaerobic processes) [11].

The by-products used in this paper for treating AMD are red mud and CFA. Red mud comes from the Bayer process [25,26], whereas coal fly ash is the inorganic residue from coal combustion. In red mud, there are mainly hematite, other crystalline aluminium silicate phases, silica, titanium oxide, rare earth oxides and un-leached residual alumina [27]. Coal fly ash contains approximately 50% of crystalline phases, mostly quartz and mullite [28].

The neutralization process enables the transformation of several waste streams into valuable products regarding the zero waste guidelines in technology. There are several water treatment methods based on red mud and CFA [29] like acid and base treated powder [30–33] or zeolites as

special aluminium silicates [34,35], but not all of them have yet been tested in acid mine drainage. Transforming CFA to zeolites can increase the adsorption of dissolved metals [36].

Our main aim is to perform a neutralization of AMD using secondary materials such as red mud and CFA and to discuss the possibility of the recovery of valuable metals such as Al, Zn, Mn and rare earth elements. The neutralization of AMD in this study is a preparation of wastewater for return into downstream processing or releasing to the environment. Acidic water can damage the plants by corroding or damaging the environment. Another aim of neutralization with alkaline material is the preparation of solid waste materials for further metal winning processes. The final aim of this study is to develop a process for water purification which fulfils the following criteria: economical, good water quality after clarification, resources of materials used for neutralization are as regionally available (<500 km) as possible and waste products are environmentally friendly.

2. Materials and Experimental Procedure

2.1. Characterisation of the Studied Materials

The AMD sample was collected from Mpumalanga, South Africa. All sampling and laboratory analysis is performed in accordance with recognized global standards such as the International Standards organization (ISO). After sampling and laboratory analysis in South Africa, all samples were sent to Germany. The AMD water was characterized by using ICP-OES analysis (SPECTRO ARCOS, SPECTRO Analytical Instruments GmbH, Kleve, Germany) and the solid samples by X-ray fluorescence, (Axios FAST, Malvern Panalytical GmbH, Kassel, Germany). The AMD was first filtrated in order to remove the formed precipitate, but AMD was not acidified. The solid samples were ground up before the X-ray diffraction analysis (XRD) analysis. Additionally, characterization of the red mud and fly ash to the X-ray powder diffraction XRD (Bruker AXS, Karlsruhe, Germany) was operated. Bauxite residue, employed during AMD-treatment as the main raw material, was provided by Aluminum of Greece plant, Metallurgy Business Unit, Mytilineos S.A. (AoG). The sample was first homogenized by using laboratory sampling procedures (riffling method) and then a representative sample was dried in a static furnace at 105 °C for 24 h. Subsequently, the material was milled using a vibratory disc mill and the sample was fully characterized.

Chemical analyses of major and minor elements were executed via the fusion method (1000 °C for 1 h with a mixture of $Li_2B_4O_7/KNO_3$ followed by direct dissolution in 10% HNO_3 solution) through a Perkin Elmer 2100 Atomic Absorption Spectrometer (AAS) (Waltham, MA, USA), a Spector Xepos Energy Dispersive X-ray Fluorescence Spectroscope (ED-XRF) (SPECTRO, Kleve, Germany), a Thermo Fisher Scientific X-series 2 Inductively Coupled Plasma Mass Spectrometer (ICP-MS) (Waltham, MA, USA) and a Perkin Elmer Optima 8000 Inductively Coupled Plasma Optical Emission Spectrometer (ICP-OES) (Waltham, MA, USA), whereas the loss of ignition (LOI) of the sample was provided by differential thermal analysis (DTA), using a SETARAM TG Labys-DS-C (Caluire, France) system in the temperature range of 25–1000 °C with a 10 °C/min-heating rate, in air atmosphere.

Mineralogical phases were detected by XRD using a Bruker D8 Focus powder diffractometer with nickel-filtered CuKα radiation (λ = 1.5405 Å) coupled with XDB Powder Diffraction Phase Analytical System version 3.107 which evaluated the quantification of mineral phases via profile fitting specifically for bauxite ore and bauxite residues.

2.1.1. Acid Mine Drainage from South Africa

The pH of the AMD wastewater ranges around 2.0. The ICP-OES analysis given in Table 1 shows the composition from the wastewater which has a dark red–yellow colour as shown in Figure 1 and their limits in the TrinkwV. According to the Ficklin diagram from [9], the AMD sample is defined as highly acidic and as having a high metal content inn the water. The total concentration of the relevant metals (mg/L), amounted to 18.903 mg. The single concentration of elements in AMD (mg/L) amounted to 14.2 Zn, 2.09 Ni, 1.94 Co, 0.65 Cu, 0.02 Cd, and 0.003 Pb. Comparison of the metal concentration

with the TrinkwV shows that the critical metals were cadmium, chromium and nickel, iron manganese and the sulphate. The pH of 2.0 was too low (interval is 6.5–9.5).

Table 1. Metal containing wastewater (three significant figures).

Substance	**$Fe^{2+/3+}$**	**Ca^{2+}**	**Mg^{2+}**	**Al^{3+}**	**Mn**
Concentration [mg/L]	2970	503	435	370	82
Limit (TrinkwV) [mg/L]	0.2	-	-	0.2	0.05
Substance	Na^{2+}	Si^{4+}	Zn^{3+}	Ce^{3+}	Ni^{2+}
Concentration in [mg/L]	52.4	44.6	14.3	5.51	2.09
Limit (TrinkwV) [mg/L]	-	-	-	-	0.02
Substance	Y^{3+}	Co^{2+}	Nd^{3+}	La^{3+}	Cu^{2+}
Concentration in [mg/L]	2.05	1.94	1.31	0.85	0.65
Limit (TrinkwV) [mg/L]	-	-	-	-	2
Substance	Cr^{3+}	Sc^{3+}	Cd^{2+}	Pb^{2+}	SO_4^{2-}
Concentration in [mg/L]	0.15	0.11	0.02	0.003	10,200
Limit (TrinkwV) [mg/L]	0.05	-	0.003	0.01	250

Figure 1. Mine drainage water from South Africa.

2.1.2. Red Mud from Germany and Greece

For the neutralisation experiments, wto sorts of red mud were used. In Figure 2, the red mud shown on the left originates from Germany (Stade, Lower Saxony, Germany), and the right one was from Greece (Aluminium of Greece, Viotia). The Greek red mud is darker due to its higher content of iron as shown in Table 2. This table shows that the Greek red mud contains more iron oxide, alumina and lime than the sample from Germany. In contrast, the German sample contains more sodium oxide, titanium dioxide and silica. Red mud is very alkaline due to the sodium hydroxide from the Bayer process (pH < 12). For further experiments, the s/L-rates of 1:10 (100 g/L AMD) and 1:5 (200 g/L AMD) were chosen.

Table 2. Content of oxides in the red mud samples wt.% or ppm (Sc).

Origin	**Fe_2O_3**	**Al_2O_3**	**CaO**	**SiO_2**	**TiO_2**	**Na_2O**	**Cr_2O_3**	**Sc**
Germany	35.3	15.7	6.7	14.0	11.4	8.9	0.2	86
Greek	44.0	23.0	10.2	5.5	5.6	1.8	0.3	122

Figure 2. Red mud samples, (**left**) from Germany, (**right**) from Greece.

The XRD analysis of Greek Red Mud is presented in Table 3.

Table 3. X-ray diffraction analysis (XRD) analysis of Greek red mud (d = 1.87 μm).

Mineralogical Phase	(wt.%)
Cancrinite [$Na_6Ca_{1.5}Al_6Si_6O_{24}(CO_3)_{1.6}$]:	15.0
Perovskite [$CaTiO_3$]	4.5
Hematite [Fe_2O_3]:	30.0
Boehmite [AlO(OH)]:	3.0
Goethite [FeO(OH)]:	9.0
Anatase [TiO_2]:	0.5
Andradite [Ca–Fe–Al–Si oxides]:	17.0
Quartz [SiO_2]:	2.0
Rutile [TiO_2]:	0.5
Calcite [$CaCO_3$]:	4.0
Chamosite [$(Fe^{2+},Mg)_5Al(AlSi_3O_{10})(OH)_8$]:	4.0
Diaspore [AlO(OH)]:	9.0
Gibbsite [$Al(OH)_3$]:	2.0
Total	98.5

The XRF analysis of the rare earth elements in Greek red mud is shown in Table 4.

Table 4. Composition of rare earth elements in Greek red mud.

Elements	Y	La	Ce	Pr	Nd	Sm	Eu	Gd
(g/t)	76	114	368	28	99	21	5	22
Elements	Dy	Ho	Er	Tm	Yb	Lu	Y	Tb
(g/t)	17	4	13	2	14	2	80	3

Mineralogical analysis of the German red mud was explained by Kaussen and Friedrich [37]. The missing 1.5% accounts for unaccounted, unknown or amorphous content. There is no sufficient reference data (known crystallographic measurements) to characterize 100% of bauxite residue

mineralogical composition. In the current XDB full profile fitting mineral phase quantification it was not possible to quantify amorphous content. Amorphous content can be determined in phase quantification when a known quantity of an internal standard such as corundum is added to the sample.

2.1.3. Coal Fly Ash from South Africa

The coal fly ash used in this study was obtained from an Eskom thermal power station, Mpumalanga, South Africa. The XRD analyses of fly ashes have been measured with a Bruker D4 powder diffractometer in Bragg–Brentano geometry. The qualitative evaluation was done with the program EVA and the PDF 2 file from ICSD. The quantitative determination was carried out using a Rietveldt refinement with the program TOPAS from Bruker. The analyses were carried out on powders <60 µm which were prepared as backloading compacts. SEM-analysis was performed using GEMINI SEM 300, Car Zeiss Microscopy GmbH; Oberkochen, Germany.

As shown in Table 5, the main components of fly ashes are silica, alumina, lime and hematite with a sum of 96.1 wt.%, and Y_2O_3 in small amounts (0.013). X-ray diffraction shows that 49% of the phases are amorphous phases, and the proportion of crystalline phase is (in %): 0.3 CaO, 0.7 Fe_2O_3, 38 Al_4SiO_8, 12 SiO_2, and 0.1 TiO_2. Most of the other oxides are present in traces. The coal fly ash in Figure 3 has a light grey colour (left) and spherical submicron particles (right).

Table 5. X-ray fluorescence (XRF) analysis of the content of compounds in the coal fly ash (wt.%).

SiO_2	Al_2O_3	CaO	Fe_2O_3	TiO_2	MgO	Na_2O
56.2	32.1	4.4	3.4	1.68	1.1	0.352
Cr_2O_3	MnO	NiO	PbO	CuO	Y_2O_3	ZnO
0.057	0.031	0.019	0.017	0.015	0.013	0.010

Figure 3. Fly ash powder (**left**) and SEM analysis (**right**).

2.2. Parameters for Neutralization

For neutralization, there are four important parameters:

- Experimental time (min): 5, 10, 20, 40, 60, 120.
- Precipitation media: coal fly ash (CFA), German red mud (GerRM), Greek red mud (GrRM)
- solid/liquid (s/L)-Ratio: 1:10, 1:5, 1:2
- Temperature (°C): 20 (room temperature), and 60 (after Heating)

The experiments, see Table 6, were designed for each media separately because coal fly ash is less alkaline, but contains yttrium (0.01%), and it is very stable for leaching. Every experiment was conducted twice to reproduce the results.

Table 6. Design of the experiment.

Factor	Low	High
s/L-rate	1:10 (RM), 1:5 (CFA)	1:5 (RM), 1:2 (CFA)
Temperature	Room temperature, 20 °C	60 °C

2.3. Setup and Test Performance

The aim of the following experiments is to prove the necessity of by-products to neutralize 500 mL of metallic wastewater. The quantity of the substances is:

- 500 mL or 1 L of defiled wastewater
- up to 200 g red mud and 250 g fly ash

The acid mine drainage was heated up to between 20 °C and 60 °C and agitated for 120 min up to 350 rpm. After precipitation, 6 samples with approximately 10 mL (from 500 mL samples) or 50 mL (from 1 L samples) were taken out of the suspension. The filtered 10 mL samples were diluted with deionised water, from a 5 mL solution samples to 50 mL, without new dilution. The solid residues were analysed after precipitation in order to determine the metal content and the absorption kinetics regarding the consumed red mud and fly ash. The precipitation and absorption fraction were calculated using Equations (4) and (5), respectively.

3. Results and Discussion

With respect to iron ions as the greatest fraction in the AMD wastewater, white and yellow flakes can be found in the samples after 5 and 10 min. In the samples with the red muds, there are white flakes, as seen Figure 4. In the samples with coal fly ash there is a yellow suspension due to a lower pH than 3 as seen in Figure 5. Yellow-orange powders are left after a second filtration of the solution. These yellow–orange flakes indicate that iron has precipitated as iron(III) hydroxide from the solution. In the red mud samples, the iron hydroxide is already removed from the red mud. The reformation of $Fe(OH)_3$ in the filtrate of coal fly ash indicates that the formation of $Fe(OH)_3$ at constant pH has a long term kinetic of several minutes.

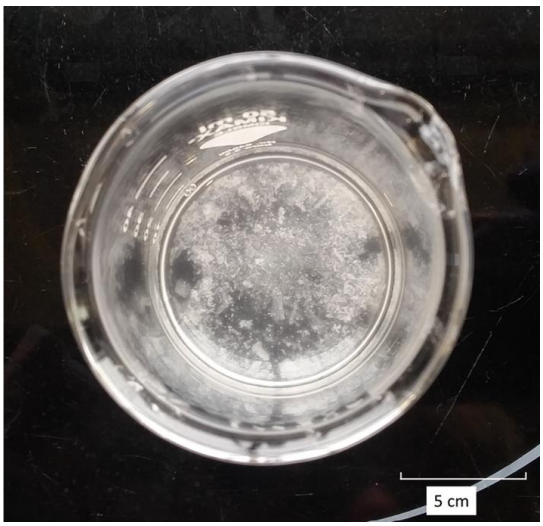

Figure 4. Typical flakes in the 5 min and 10 min samples after treatment with red mud.

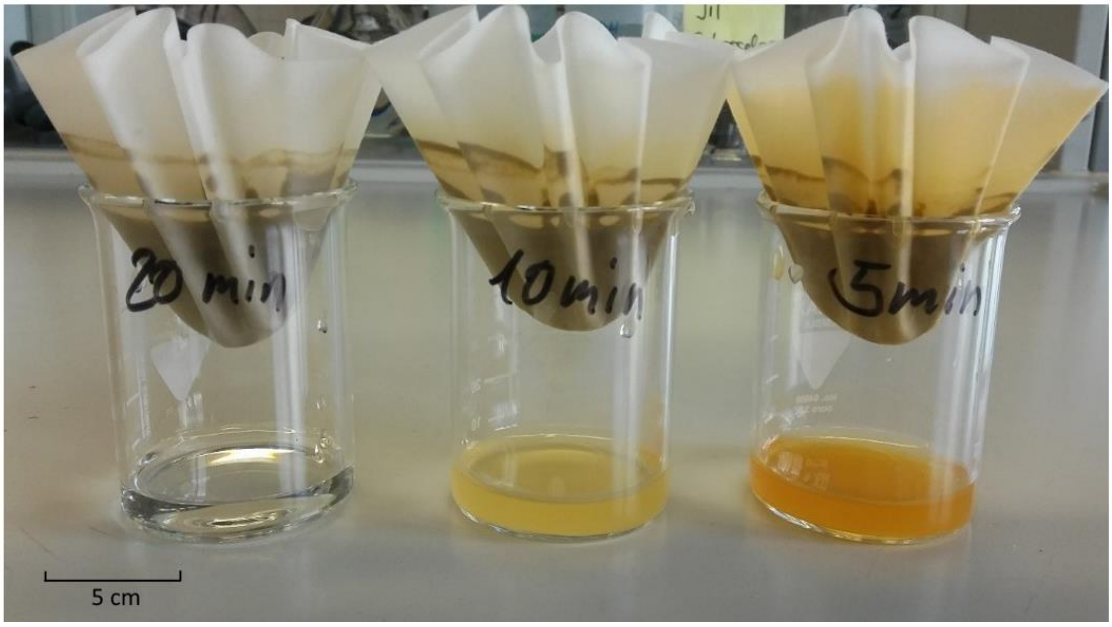

Figure 5. Suspension in the 5, 10 and 20 min samples after treatment with coal fly ash.

The XRF analysis showed that the yellow powder after treatment with coal fly ash, filtration and drying mainly contains approximately

- 30.94 ± 0.01% iron
- 11.66 ± 0.01% sulphur
- 4.577 ± 0.010% silicium
- 3.783 ± 0.015% aluminium
- 1.416 ± 0.003% calcium

We supposed that iron and aluminium precipitate as iron(III) and aluminium(III) hydroxide, respectively. Additionally, some compounds precipitate as sulphates, e.g., $CaSO_4$, because it is slightly soluble, what is presented in Figure 6. Additionally, the presence of aluminium oxide in the product was revealed.

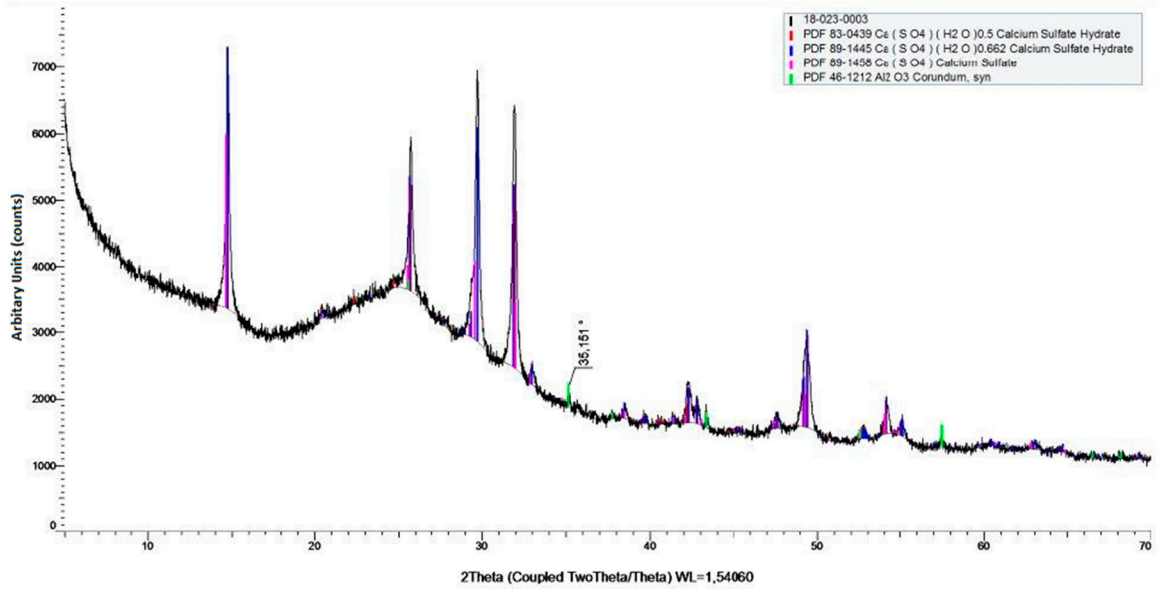

Figure 6. XRD analysis of the precipitation product.

3.1. pH Values as Function of the Time

The initial pH value of the AMD water was 1.973 ± 0.031 (the calculated relative error ΔpH/pH = 15.7%) for all 12 experiments. After the measurement of pH-Value, AMD solution was added in a glass reactor and heated to 60 °C. Red mud and fly ash (50–100 g) were added at 60 °C in the solution of AMD. The pH-Values were measured in time of 120 min. The same procedure was performed at room temperature and results were compared with ones obtained at 60 °C.

The pH was plotted as a function of time as seen in Figure 7. All samples have a strong pH increase in the first 5 min. The maximum pH of 6 can be reached by 100 g German red mud at 20 °C. The pH values from the Greek red mud tend to be lower than the ones from the German red mud, the maximum pH being 5.9, which is in the same range as the German red mud. The samples with coal fly ash indicate that in the first 5 min, the average pH was 2.78 ± 0.14 (ΔpH/pH = 5%) and most of the iron ions were still dissolved in the solution. After 10 min, the average pH was 2.93 ± 0.11 (ΔpH/pH = 4%) and there was still some iron(III) dissolved. For full iron(III) removal, the pH needs to be at least higher than three, which was mentioned by Stiefel [11].

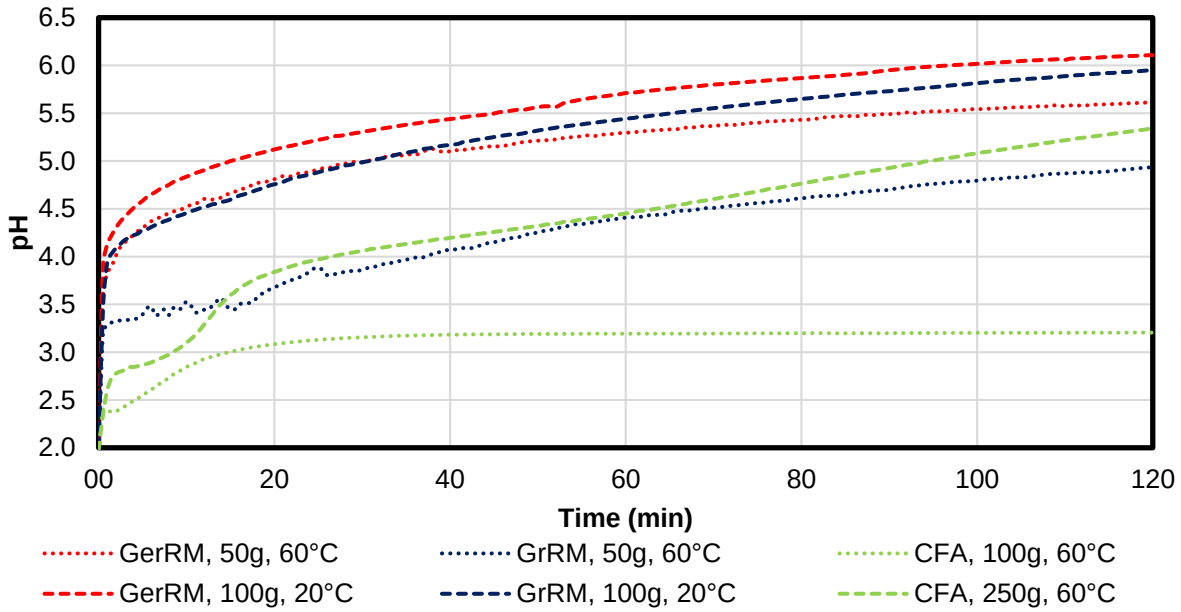

Figure 7. pH values in time (GerRM—German red mud; GrRM—Greek red mud; CFA—coal flying ash).

Coal fly ash had pH-values between 8 and 11 depending on the quantity of the added sample, in comparison to red mud (pH > 12). Especially because of 49% of amorph structure and 38% of very stable mullite in this structure, as shown at Figure 3, the fly ash has smaller neutralisation efficiency in comparison to used red mud. The temperature is very important in regards to pH measurements. As the pH value changes with the change in temperature, the new measured pH value is technically the true pH value. Under laboratory conditions, a note of the temperature and pH value should be made together. There is only one major temperature effect in pH measurement that can cause errors in readings. It is the only reasonably predictable error due to changes in temperature, and is the only temperature-related factor that a pH meter with temperature compensation can correct. This temperature error is very close to 0.003 pH/°. Generally in our experiments, Because of an influence of the diffusion of the acidic solution, an increase of temperature from room temperature to 60 °C increases the neutralization efficiency of AMD during the addition of fly ash and red mud. It seems that adding FA and RM can increase pH of AMD at the scale of 120 min. Long-term neutralization efficiency is required, as confirmed in subsequent work, and in the work of Paradis et al. [38].

3.2. Comparison of Precipitation Efficiency per Material

Regarding the literature [8], the critical pH for iron(III) precipitation using CFA can be assumed as approximately 3.0. At this point, 99% of the dissolved iron is precipitated. The maximum concentration of dissolved iron is 44.2 mg/L. However, it must be considered that the iron concentration in the solution was higher direct after the filtration since iron(III) hydroxide has precipitated after filtration. The following six figures (Figures 7–12) show the precipitation efficiency as a function of the pH of aluminium, manganese and zinc. The symbols represent the time of sampling (5, 10, 20, 40, 60, 120 min). The precipitation efficiency x_P was calculated by Equation (4). Negative values for x_P indicate leaching effects and enrichment in the acid mine drainage.

$$x_P = 1 - \frac{\text{Concentration of metal at time } t}{\text{Initial concentration of metal in AMD}} = 1 - \frac{c_t}{c_0} \quad (4)$$

3.2.1. Manganese

In Figure 8, by using the German red mud, manganese had a lower precipitation efficiency at a higher temperature (60 °C) than the sample with more mass at 20 °C at the same pH-value. There is a tendency of reaching a maximum precipitation efficiency of approximately 75% as the sample with 100 g at 20 °C, which shows a light equilibrium state. Using a Greek 50 g red mud results in leaching in acid mine drainage up to 10% at a higher temperature. Greek red mud with higher mass at room temperature leads to the precipitation of manganese up to 30%. Manganese tends to be leached in both coal fly ash experiments. In the 100 g sample at 60 °C it is leached from 10% to 22%. In the 250 g lower heated experiment, manganese was leached to 20% in the first 5 min and then precipitated until it was at a value of 6% of the initial concentration. It follows that manganese may precipitate after pH 4 by using red mud.

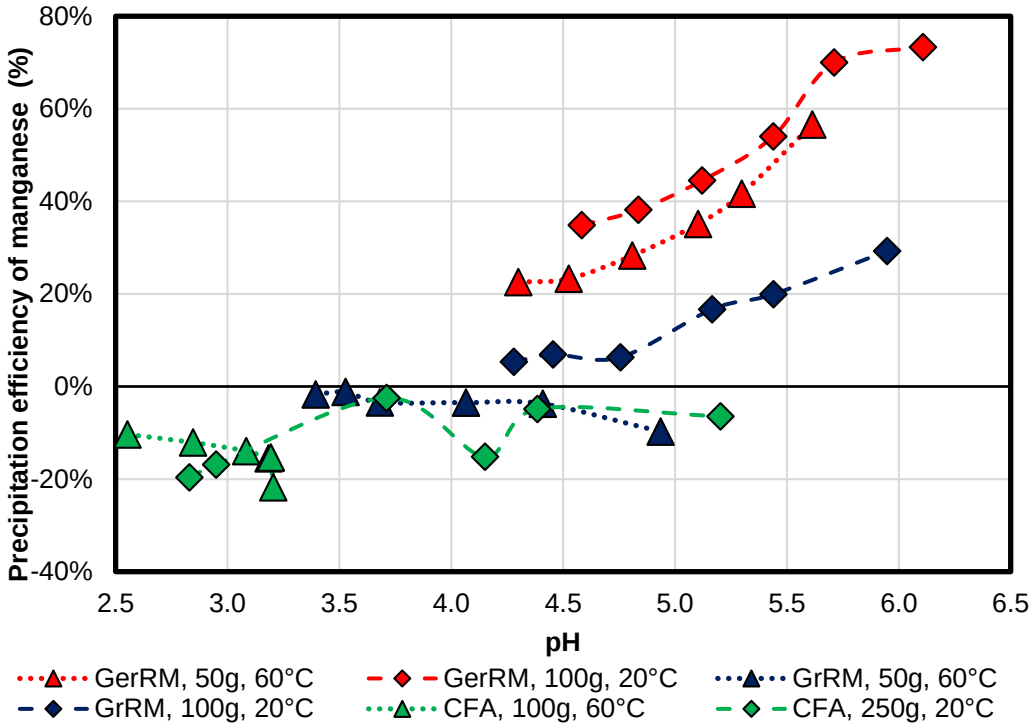

Figure 8. Participation efficiency of manganese.

3.2.2. Aluminium

Figure 9 shows the precipitation efficiency of aluminium for all precipitation media compared to the initial concentration of 370 mg/L. German red mud removes 99% of the aluminium as aluminium

hydroxide at pH 5.0. Higher temperature leads to an earlier precipitation pH and therefore, to higher efficiency at the same pH compared to the experiment with higher mass at 20 °C. As a contrast, higher mass results in faster pH increase so that the pH is higher after the same time. Experiments with Greek red mud showed a similar tendency, although the precipitation efficiency of the sample in heated acid mine drainage was just 14% after 5 min. In all coal fly ash samples, the aluminium was not precipitated under pH 3.5. In the experiment with heated acid mine drainage, a leaching from coal fly ash up to 89% at pH 2.8 occurred at first, then re-precipitation. As a conclusion, all samples showed similar correlation of pH and precipitation efficiency, like an s-curve with a strong increase between pH 3.0–3.6 in all experiments, see the red circle. Positive precipitation efficiency starts at pH 3.3–3.5 until pH-Value of 5. After the pH of 5.0, precipitation of aluminum is complete.

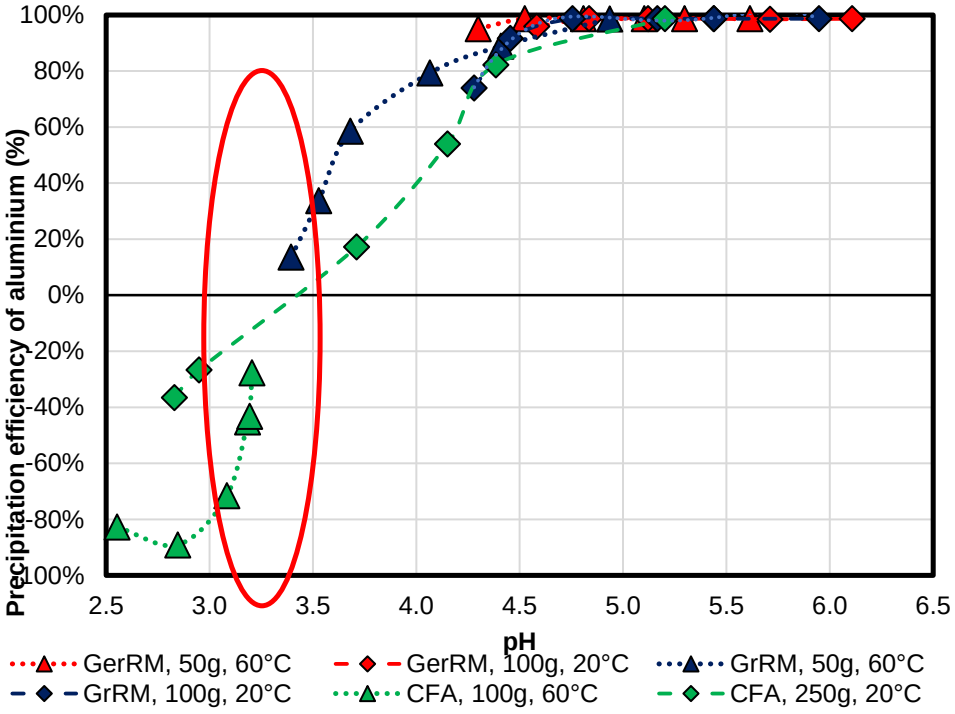

Figure 9. Participation efficiency of aluminium.

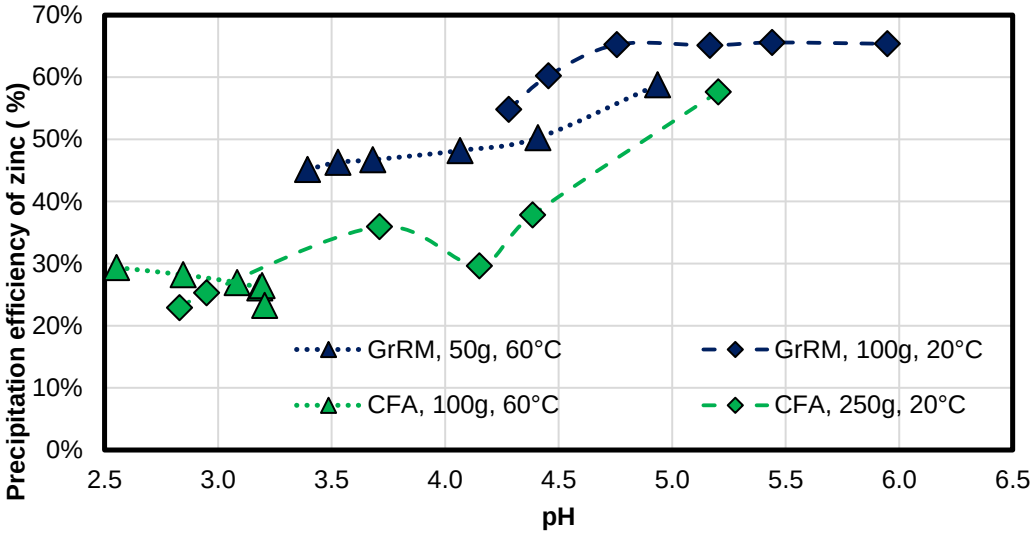

Figure 10. Participation efficiency of zinc.

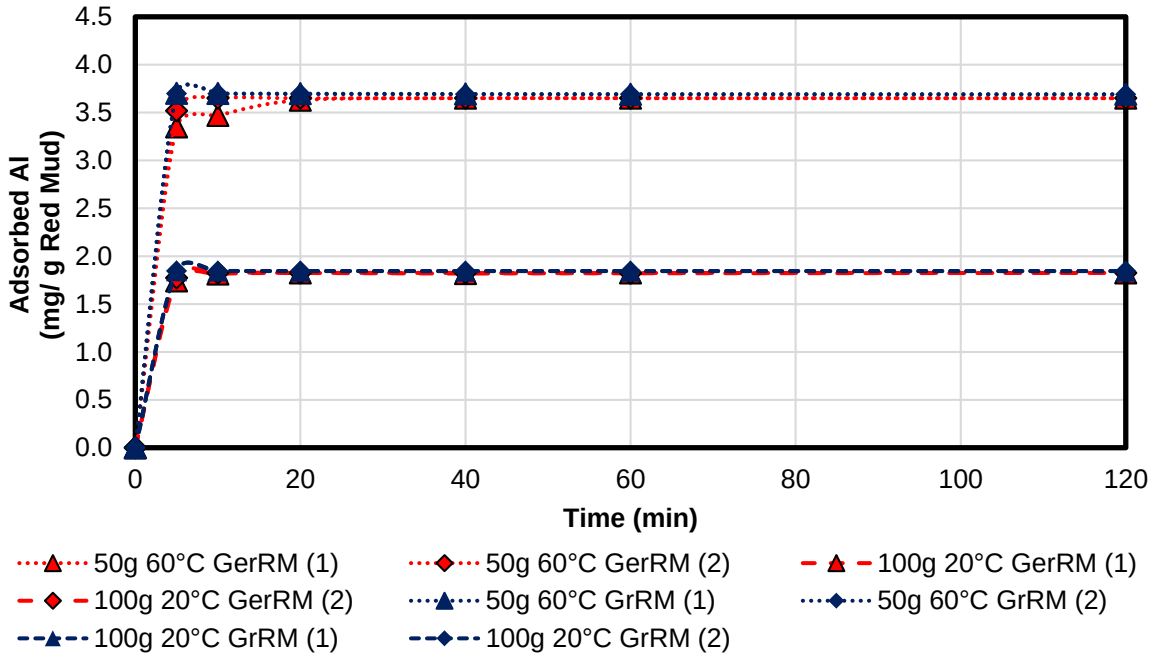

Figure 11. Kinetics of aluminium adsorption for both red muds [mg/g].

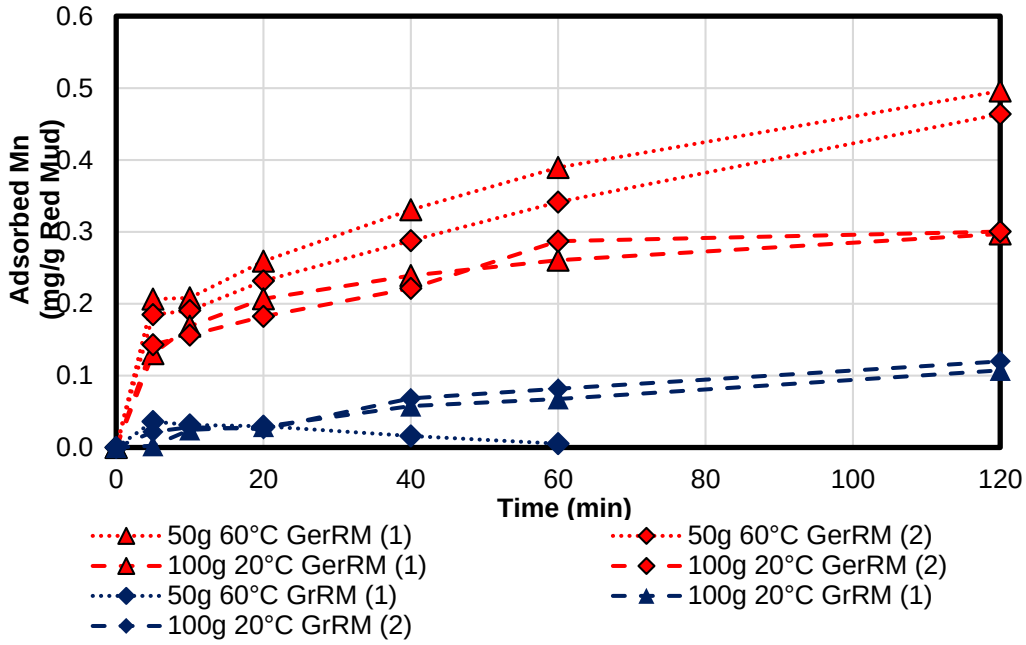

Figure 12. Kinetics of manganese adsorption for both types of red muds [mg/g].

3.2.3. Zinc

In German red mud, the zinc is completely precipitated, to under the detection limit. Zinc, as shown in Figure 10, can reach a minimum precipitation of 45% in both combinations of Greek red mud. The maximum precipitation efficiency can be at least 65% for the sample at 20 °C with 100 g and 59% for the pre-heated acid mine drainage experiment with 50 g Greek red mud. In coal fly ash, zinc was precipitated between 20% and 60% in both cases, whereas the non-heated sample had a better efficiency of 60% after 120 min. There is a linear correlation between pH and precipitation efficiency. As a conclusion, pre-heated acid mine drainage results in leaching of all metals, which is also expected of zinc but only for the first 40 min, longer neutralization leads to stronger zinc back-dissociation.

3.3. Adsorption Kinetics of Adsorbed Metals

The adsorption kinetics can be compared by using the rate of adsorbed material per gram precipitation media, see Equation (5).

$$q_t = \frac{(c_0 - c_t)_{Me} \cdot V_{\mathrm{AMD}}}{m_{\mathrm{RM/CFA}}} \quad (5)$$

with:

q_t rate of adsorbed material [mg/g]
c_0, c_t concentration of the metal ions [mg/L] (c_0: initial, c_t: after t min)
V_{AMD} volume of the tested AMD water [L]
$m_{\mathrm{RM/CFA}}$ mass of the used precipitation media [g]

3.3.1. Aluminium

Figure 11 shows the adsorption kinetics for the aluminium in the acid mine drainage precipitated by the both types of red muds. The coal fly ash samples were missing due to enrichment in the AMD. The aluminium in the ash may be a soluble phase. The concentration of aluminium in the solution was 370 mg/L, therefore there were 185 mg dissolved in 500 mL. It can be recognised that the adsorption potential was higher using red mud at 60 °C than at 20 °C. This indicates that the aluminium adsorption is a temperature-activated process and therefore, it is more like chemisorption than physisorption. The increase to 60 °C doubles the adsorption potential per gram red mud from 1.8 mg/g (0.9% of the total amount of dissolved aluminium in solution) to 3.7 mg/g (2%). The difference between the use of the German red mud and the Greek red mud was relatively small, Greek red mud was a little bit better than the German type. In case of the 50 g 60 °C sample, the mass of the adsorbed part was 185 mg, which was the maximum, whereas the 100 g 20 °C adsorbed only 180 mg. In the case of aluminium, both combinations achieved equal precipitation efficiency of 100%. After 20 min (average pH = 4.751 ± 0.495), the precipitation can be assumed as completed.

3.3.2. Manganese

The concentration of manganese was 82 mg/L which means 41 mg in 500 mL acid mine drainage water. The adsorption kinetics for manganese in Figure 12 show that the German red mud had better adsorption potential than the Greek one. Because of enrichment, the 50 g sample at 20 °C with the Greek red mud is missing, see Equation (6).

$$\mathrm{MnO} \rightarrow \mathrm{Mn^{2+}} + \mathrm{O^{2-}} \quad (6)$$

None of the samples have achieved the equilibrium state. The German red mud 100 g and 20 °C sample could have an equilibrium at 0.31 mg/g manganese. One gram can adsorb 0.7% of the dissolved manganese which is in total 30 mg (73% in total). For the German red mud 50 g at 60 °C sample, it can be assumed that the equilibrium is approximately 0.6 mg/g red mud which means an adsorption grade of 1.4% and therefore, 30 mg in total (also 73% in total). This means that both combinations can work equally for manganese, see Table 7. The equilibrium for the 50 g Greek red mud sample at 60 °C was negative due to leaching effects. Therefore, the 120 min adsorption rate cannot be determined exactly. Under recognition of instrumental errors, the equilibrium can be near zero.

Table 7. Adsorption kinetics of manganese by red mud with the percentage at assumed equilibrium.

Sample	GerRM 50/60	GerRM 100/20	GrRM 50/60	GrRM 100/20
rate in mg/g	~0.6	~0.31	~0	~0.15
% per gram	~1.4	~0.7	~0	~0.4
mass [mg]	~30	~30	~0	~15
% in total	~73	~73	~0	~37

3.3.3. Zinc

Figure 13 shows the sorption kinetic of zinc. The concentration of dissolved zinc was 14.3 mg/L, therefore, there were 7.15 mg dissolved in acid mine drainage. The equilibrium of zinc for coal fly ash was between 0.01 and 0.02 mg/g which were at a maximum 0.28% of the total amount of the dissolved zinc per gram in coal fly ash. The 100 g of coal fly ash could adsorb a maximum 2 mg which is 28% of the total amount and 250 g maximum 5 mg zinc (nearly 70% of the total zinc). For Greek red mud, the equilibrium at 20 °C was approximately 0.047 mg/g which is a grade of 0.66%. A 100 g portion of this sample can adsorb 4.7 mg zinc which is 66% of the total zinc in solution. The best sample with 50 g and 60 °C had a short equilibrium 0.067 mg/g for 15 min which was 0.9% adsorption per gram with total adsorption of 3.35 mg (47%) zinc. After 20 min, an increase of adsorption can be seen. This indicates that there could be another mechanism of adsorption, like precipitation. After 40 min, the mixture achieved a pH of 4.1. Regarding the results, the Greek red mud had a better adsorption potential than the coal fly ash but overall, the 250 g coal fly ash sample at 20 °C can be as useful as the 100 g of Greek red mud at 20 °C, as shown in Table 8. The precipitation follows Equation (7).

$$Zn^{2+} + 2OH^{-} \rightarrow Zn(OH)_2 \quad (7)$$

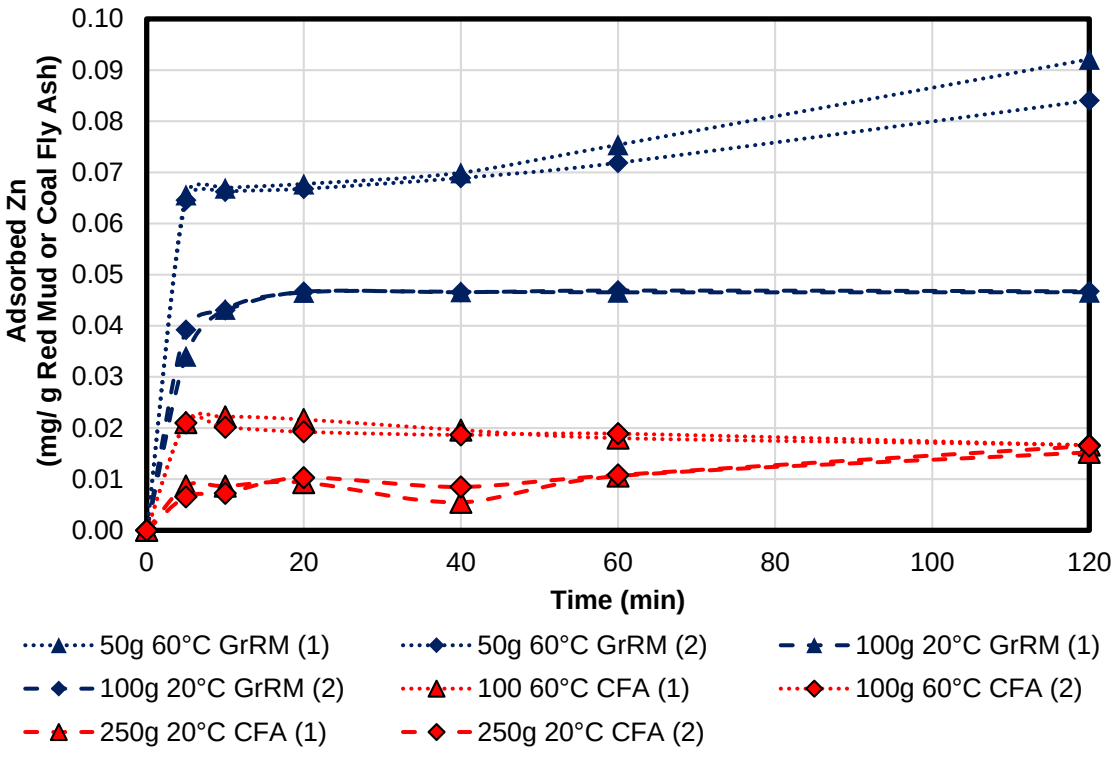

Figure 13. Kinetics of zinc adsorption for Greek red mud and coal fly ash [mg/g].

Table 8. Kinetics of zinc adsorption for Greek red mud and coal fly ash.

Sample	GrRM 50/60	GrRM 100/20	CFA 100/60	CFA 250/20
rate [mg/g]	>0.067	0.047	~0.02	~0.02
% per gram	>0.94	0.66	~0.28	~0.28
mass [mg]	>3.35	4.7	~2	~5
% in total	>47	66	~28	~70

3.4. Leaching Kinetics

Analogously, the leaching kinetics can be calculated with Equation (8) as well as the adsorption kinetics in the previous chapter.

$$q_t = \frac{(c_t - c_0)_{Me} V_{\mathrm{AMD}}}{m_{\mathrm{RM/CFA}}} \tag{8}$$

Sodium

Due to a high concentration of sodium hydroxide, it is the main component for neutralization of acid mine drainage. The consumption of sodium from coal fly ash for neutralization of AMD was not very high, only approximately 0.05 mg/g coal fly ash since the content of sodium in coal fly ash was just 0.35 wt.% (<1 mg/g), whereas the German red mud contains 8.9 wt.% (66 mg/g) and the Greek red mud 1.8 wt.% (13 mg/g). Regarding the average leaching kinetics of sodium in Figure A1 in Appendix A, German red mud at 60 °C has the highest leaching ability with 50 mg/g sodium which is 76% of total sodium in the sample as seen in Table 9 and 20 mg/g in the non-heated sample which was 30%. The heated Greek red mud had a similar leaching ability like the non-heated German red mud with 20 mg/g. The non-heated Greek red mud had a leaching ability of 10 mg/g which was 77% of the total sodium in the sample. As a conclusion, the non-heated German red mud and the heated Greek red mud sample have a similar ability to achieve the same neutralization pH per gram.

$$\mathrm{NaOH} \rightarrow \mathrm{Na^+} + \mathrm{OH^-} \tag{9}$$

Table 9. Content of sodium at the beginning and after leaching in the types of red mud.

Sample	GerRM 50/60	GerRM 100/20	GrRM 50/60	GrRM 100/20
Sodium in solid [mg/g]	66	66	13	13
Leached sodium [mg/g]	50	20	20	10
Percentage [%]	76	30	(153)	77

3.5. Rare Earth Concentration in the One Litre Experiments

The initial concentration of cerium is 5.51 mg/L and of yttrium was 2.05 mg/L. Figure 14 and Table 10 shows the concentration of the rare earth elements yttrium and cerium during the experiments. The detection limit for the rare earths was 1.0 mg/L, which marks the start of the *y*-axis. The rare earth elements (yttrium and cerium) were adsorbed by Greek red mud with an efficiency of 50% and 80% at 60 °C in 5 min, respectively. After 5 min, using German red mud can reduce the concentration of the rare earth to nearly under the detection limit (Ce: 1.12 mg/L, Y: <1 mg/L). Using Greek red mud reduces cerium to under the detection limit after 60 min, yttrium after 40 min. Using coal fly ash can result in re-dissolving into acid mine drainage which indicates an equilibrium of the concentration in the solid and in the acid mine drainage. After 60 min, the concentration of the rare earths does not change much. There is a steady-state in concentration.

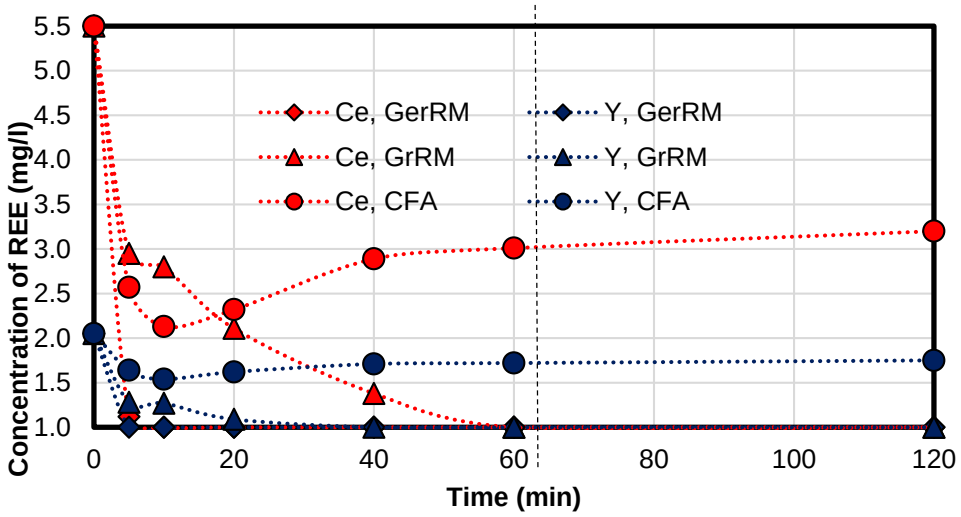

Figure 14. Concentration of yttrium and cerium in time.

Table 10. Yttrium and cerium in precipitation experiment [mg/L].

Time [min]	5	10	20	40	60	120
Ce, GerRM	1.12	<1	<1	<1	<1	<1
Y, GerRM	<1	<1	<1	<1	<1	<1
Ce, GrRM	2.95	2.80	2.11	1.38	<1	<1
Y, GrRM	1.28	1.27	1.09	< 1	<1	<1
Ce, CFA	2.57	2.13	2.32	2.89	3.01	3.20
Y, CFA	1.64	1.54	1.62	1.71	1.72	1.75

3.6. Sodium Concentration Regarding the Guidelines

The initial concentration of the sodium in acid mine drainage is 52.4 mg/L. The guideline for sodium in drink water is 200 mg/L [21], see the red line in Figure A2 in Appendix A. The German red mud leads to a final concentration of 4–5 g/L which is twenty-five times that of the recommended concentration. The final concentration of the Greek red mud was approximately 2 g/L which is tenfold of the recommended concentration. Only the coal fly ash sample fit into the guideline, with a final concentration of approximately 70 mg/g. Therefore, for the red mud samples, it is necessary to distinguish if the water is used as drink water after treatment.

With respect to the results, there is a possibility of purifying the acid mine drainage by precipitation with red mud and coal fly ash. Overall iron is removed nearly completely, and aluminium also precipitates to 99% in most samples. Same samples as Greek red mud and coal fly ash have a potential for selective removal of metals which can be useful for multistage process designing. In all red mud samples, the concentration of sodium has increased strongly.

Comparison of the adsorption kinetics shows that in some cases, the combinations of higher mass or higher temperature could give similar results like those in the experiment with German red mud and manganese (both 73% of total) or the one with both kinds of red muds and aluminium. Additionally, for zinc precipitation, the 100 g, 20 °C Greek red mud and the 250 g, 20 °C coal fly ash have equal precipitation efficiency. For economical use, higher mass and low temperature are preferred. Additionally, the red mud and the coal fly ash can replace the soil, which enables outside application for neutralisation. The neutralised red mud and coal fly ash can be used for further metal-winning treatment.

The main cause for the increase of pH is the sodium hydroxide. Since the red mud can release up to 80% of the sodium ions into acid mine drainage, a pH increase up to 6 is possible. A combination of

higher mass and higher temperature can achieve the neutral water state. The coal fly ash causes pH increase by dissociation of metal oxides in acids, but the pH increase is not as high as using red mud since coal fly ash does not contain sodium oxide. The oxides release oxygen to acid mine drainage, which influences the potential of acid mine drainage, resulting in the formation of hydroxyl ions and shifts the precipitation pH to lower values.

The total amount of the rare earth elements was 9.83 mg/L, which can be reduced after neutralization under 4 mg/L using German red mud.

The German red mud performs the best results of all media. The Greek red mud also has good results, but they were not as good as the German ones. The precipitation efficiency of coal fly ash was low in some samples. Coal fly ash is usable when iron, aluminium and zinc needs to be precipitated but manganese would be dissolved in solution.

4. Conclusions

The following conclusions are found in this work:

- In all samples, the iron is removed after a pH of 3.0 (20 min) from acid mine drainage, and aluminum after a pH of 5.0.
- The required pH for drinking water (pH > 6.5) can be nearly reached.
- Higher mass of red mud and flying ash leads to higher final pH.
- In all experiments, the German red mud achieved the highest pH values.
- Because of it's high alkaline nature (pH > 12), German red mud is the best precipitation media for iron, aluminium, cerium and yttrium.
- The red muds removed the metals but enriches the dissolved sodium.
- Sample with coal fly ash enriches the acid mine drainage with sodium and zinc since sodium is contained in low concentrations.
- Increase of temperature can increase adsorption kinetics.
- Under a pH of 3, yellow flakes have precipitated in the filtrate. The flakes contain iron(III) hydroxide.
- White flakes indicate the precipitation of aluminum(III) hydroxide.

Kinetic study shows that contrast combinations of mass and temperature can achieve the same precipitation adsorption. Increasing of temperature to 60 °C can double the adsorption capacity of material like aluminium, which is equivalent to the twofold mass of material. The alternative with the higher amount of material should be preferred because of the higher pH increase due to easily-soluble sodium hydroxide. As the results indicated, there is much less metal removal from solution using the adsorption method.

Author Contributions: Conceptualization, B.X., V.K. and S.S.; Funding acquisition, S.N. and B.F.; Investigation, V.K., Y.M. and B.M.; Methodology, V.K., S.S. and B.X.; Supervision, S.N., G.S.S. and B.F.; Writing—original draft, S.S., B.X., S.N., B.M., G.S.S. and B.F. All authors have read and agreed to the published version of the manuscript.

Funding: This research was funded by the International Office of the BMBF in Germany, grant number. 01DG17024, and by NRF in South Africa (grant number: GERM160705176077). The APC was funded by the International Office of the BMBF in Germany, grant number. 01DG17024.

Conflicts of Interest: The authors declare no conflict of interest.

Appendix A

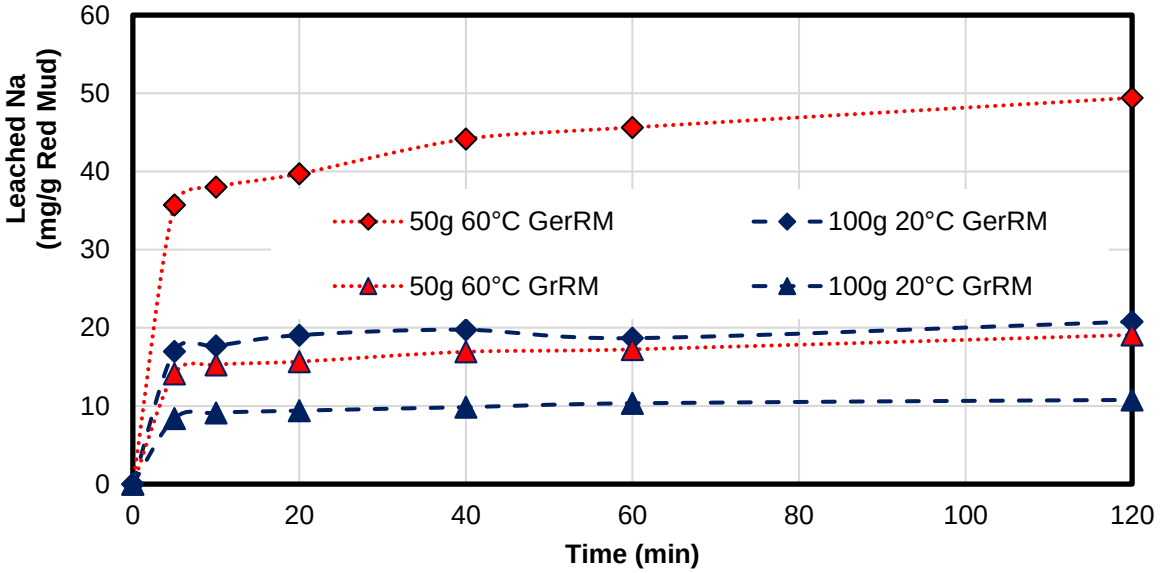

Figure A1. Kinetics of sodium adsorption for German and Greek red mud [mg/g].

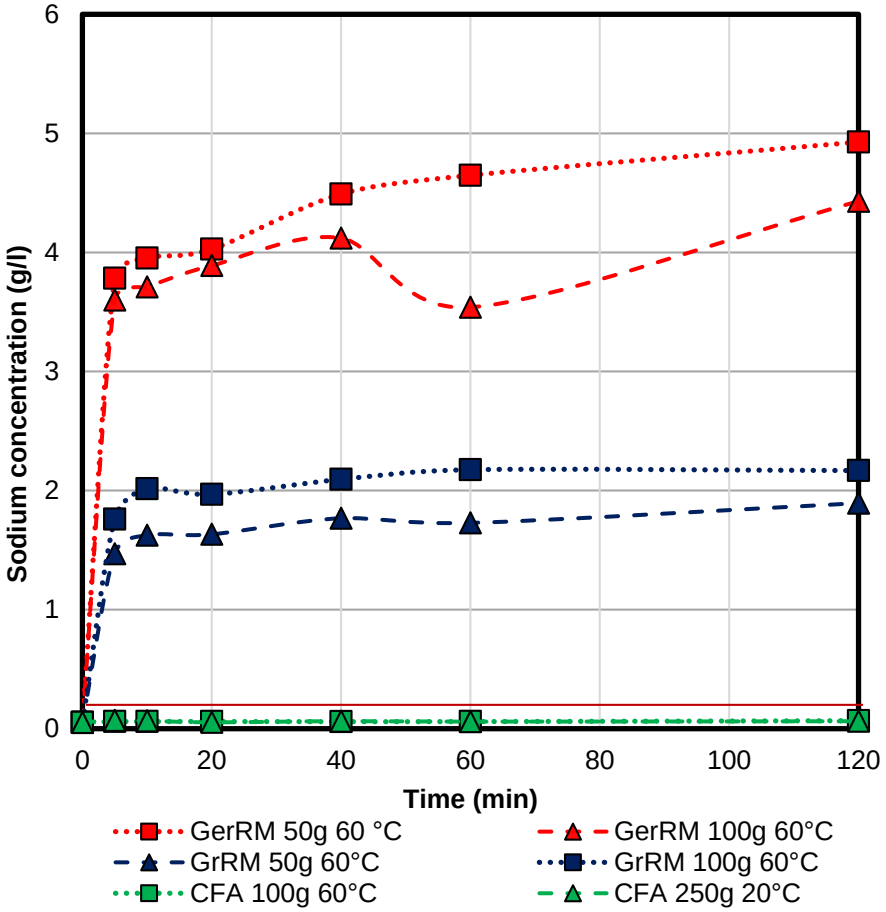

Figure A2. The concentration of sodium in treated acid mine drainage regarding the guidelines [18].

References

1. WHG. *Gesetz zur Ordnung des Wasserhaushalts*; German Federal Ministry of Justice and Consumer Protection: Berlin, Germany, 2009.
2. Knight, J.; Rogerson, C.M. *The Geography of South Africa*, 1st ed.; Springer: Cham, Switzerland, 2019; pp. 27–31.
3. Mccarthy, T.S. The impact of acid mine drainage in South Africa. *S. Afr. J. Sci.* **2011**, *107*, 5–6. [CrossRef]
4. Tabelin, C.B.; Igarashi, T.; Tabelin, M.V.; Park, I.; Opiso, E.M.; Ito, M. Arsenic, selenium, boron, lead, cadmium, copper, and zinc in naturally contaminated rocks: A review of their sources, modes of enrichment, mechanisms of release, and mitigation strategies. *Sci. Total Environ.* **2018**, *645*, 1522–1553. [CrossRef] [PubMed]
5. Park, I.; Tabelin, C.B.; Jeon, S.; Li, X.; Seno, K.; Ito, M.; Hiroyoshi, N. A review of recent strategies for acid mine drainage prevention and mine tailings recycling. *Chemosphere* **2019**, *219*, 588–606. [CrossRef] [PubMed]
6. Igarashi, T.; Herrera, P.S.; Uchiyama, H.; Miyamae, H.; Iyatomi, N.; Hashimoto, K.; Baltazar, C.B.T. The two-step neutralization ferrite-formation process for sustainable acid mine drainage treatment: Removal of copper, zinc and arsenic, and the influence of coexisting ions on ferritization. *Sci. Total Environ.* **2020**, *715*, 136877. [CrossRef] [PubMed]
7. Bwapwa, J.K. A Review of Acid Mine Drainage in a Water-Scarce Country: Case of South Africa. *Environ. Manag. Sustain. Dev.* **2018**, *7*, 1–20. [CrossRef]
8. Singer, P.C.; Stumm, W. Acidic Mine Drainage: The Rate-Determining Step. *Science* **1970**, *167*, 1121–1123. [CrossRef]
9. Plumlee, G.S.; Smith, K.S.; Montour, M.R.; Ficklin, W.H.; Mosier, E.L. Geologic Controls on the Composition of Natural Waters and Mine Waters Draining Diverse Mineral-Deposit Types. In *The Environmental Geochemistry of Mineral Deposits. Reviews in Economic Geology*; Society of Economic Geologists: Littleton, CO, USA, 1999; Chapter 19; Volume 6, pp. 373–435.
10. Lim, J.; Yu, J.; Wang, L.; Jeong, Y.; Shin, J.H. Heavy Metal Contamination Index Using Spectral Variables for White Precipitates Induced by Acid Mine Drainage: A Case Study of Soro Creek. *IEEE Trans. Geosci. Remote Sens.* **2019**, *57*, 1–19. [CrossRef]
11. Stiefel, R. *Abwasserrecycling: Technologien und Prozesswassermanagement: Das Konzept Prozesswasserautarkie*, 1st ed.; Springer: Wiesbaden, Germany, 2017; p. 104.
12. Smit, J.P. *The Treatment of Polluted Mine Water, Presented at the Mine, Water and Environment*; International Mine Water Association: Sevilla, Spain, 1999.
13. Dietrich, G. *Hartinger Handbuch Abwasser und Recyclingtechnik*, 3rd ed.; Carl Hanser Verlag: München, Germany, 2017; pp. 57–68, 102, 113–118.
14. Baur, A.; Fritsch, P.; Hoch, W.; Merkl, G.; Rautenberg, J.; Weiß, M.; Wricke, B. *Mutschmann/Stimmelmayr Taschenbuch der Wasserversorgung*, 17th ed.; Springer: Wiesbaden, Germany, 2019; pp. 5, 236, 252, 258, 286–300, 312–317, 327–332.
15. Crane, R.A.; Sapsford, D.J. Selective formation of copper nanoparticles from acid mine drainage using nanoscale zerovalent iron particles. *J. Hazard. Mater.* **2018**, *347*, 252–265. [CrossRef]
16. Asokbunyarat, V.; van Hullebusch, E.D.; Lens, P.N.L.; Annachhatre, A.P. Immobilization of Metal Ions from Acid Mine Drainage by Coal Bottom Ash. *Water Air Soil Pollut.* **2017**, *228*, 328. [CrossRef]
17. Sawyer, C.N. *Chemistry for Environmental Engineering and Science*, 5th ed.; McGraw-Hill: New York, NY, USA, 2003; p. 99.
18. Paradis, M.; Duchesne, J.; Lamontagne, A.; Isabel, D. Long-term neutralisation potential of red mud bauxite with brine amendment for the neutralisation of acidic mine tailings. *Appl. Geochem.* **2007**, *22*, 2326–2333. [CrossRef]
19. World Health Organization. *Guidelines for Drinking-Water Quality*, 4th ed.; World Health Organization: Geneva, Switzerland, 2011; pp. 223–228.
20. German Federal Ministry of Justice and Consumer Protection. *Verordnung über Anforderungen an das Einleiten von Abwasser in Gewässer*; AbwV, German Federal Ministry of Justice and Consumer Protection: Berlin, Germany, 1997.
21. German Federal Ministry of Justice and Consumer Protection. *Verordnung über die Qualität von Wasser für den Menschlichen Gebrauch*; TrinkwV, German Federal Ministry of Justice and Consumer Protection: Berlin, Germany, 2001.

22. Christen, D.S. *Praxiswissen der chemischen Verfahrenstechnik: Handbuch für Chemiker und Verfahrensingenieure*, 2nd ed.; Springer: Berlin/Heidelberg, Germany, 2010; pp. 333–366.
23. Kurzweil, P. *Chemie: Grundlagen, Aufbauwissen, Anwendungen und Experimente*, 10th ed.; Springer: Wiesbaden, Germany, 2015; pp. 177–178.
24. German Federal Environment Agency. *Bekanntmachung der Liste der Aufbereitungsstoffe und Desinfektionsverfahren gemäß § 11 der Trinkwasserverordnung—20. Änderung—(Stand: Dezember 2018)*; German Federal Environment Agency: Dessau-Roßlau, Germany, 2018.
25. Mortimer, C.E.; Müller, U. *Chemie*, 9th ed.; Georg Thieme Verlag KG: Stuttgart, Germany, 2007; p. 475.
26. Kammer, C. *Aluminium Taschenbuch Band 1: Grundlagen und Werkstoffe*, 16th ed.; Aluminium: Düsseldorf, Germany, 2002; pp. 20–25.
27. Castaldi, P.; Silvetti, M.; Santona, L.; Enzo, S.; Melis, P. XRD, FTIR, and Thermal Analysis of Bauxite Ore-Processing Waste (Red Mud) Exchanged with Heavy Metals. *Clays Clay Miner.* **2008**, *56*, 461–469. [CrossRef]
28. Kutchko, B.G.; Kim, A.G. Fly ash characterization by SEM–EDS. *Fuel* **2006**, *85*, 2537–2544. [CrossRef]
29. Ahmed, M.J.K.; Ahmaruzzaman, M. A review on potential usage of industrial waste materials for binding heavy metal ions from aqueous solutions. *J. Water Process. Eng.* **2016**, *10*, 39–47. [CrossRef]
30. Smičiklas, I.; Smilijanic, S.; Peric, A.-G.; Sljivic, M.-I.; Mitric, M.; Antonovic, D. Effect of acid treatment on red mud properties with implications on Ni(II) sorption and stability. *Chem. Eng. J.* **2014**, *242*, 27–35. [CrossRef]
31. Sahu, M.K.; Mandal, S.; Dash, S.S.; Badhai, P.; Patel, R.K. Removal of Pb(II) from aqueous solution by acid activated red mud. *J. Environ. Chem. Eng.* **2013**, *1*, 1315–1324. [CrossRef]
32. Nadaroglu, H.; Kalkan, E.; Demir, N. Removal of copper from aqueous solution using red mud. *Desalination* **2010**, *251*, 90–95. [CrossRef]
33. Visa, M.; Isac, L.; Duta, A. Fly ash adsorbents for multi-cation wastewater treatment. *Appl. Surf. Sci.* **2012**, *258*, 6345–6352. [CrossRef]
34. Qiu, W.; Zheng, Y. Removal of lead, copper, nickel, cobalt, and zinc from water by a cancrinite-type zeolite synthesized from fly ash. *Chem. Eng. J.* **2009**, *145*, 483–488. [CrossRef]
35. Smart, L.E.; Moore, E.A. *Solid State Chemistry—An Introduction*, 3rd ed.; Taylor & Francis Group: Boca Raton, FL, USA, 2005; p. 301.
36. Prasad, B.; Kumar, H. Treatment of Lignite Mine Water with Lignite Fly Ash and Its Zeolite. *Mine Water Environ.* **2019**, *38*, 24–29. [CrossRef]
37. Kaussen, F.; Friedrich, B. Phase characterization and thermochemical simulation of (landfilled) bauxite residue ("red mud") in different alkaline processes optimized for aluminum recovery. *Hydrometallurgy* **2018**, *176*, 49–61. [CrossRef]
38. Paradis, M.; Duchesne, J.; Lamontagne, A.; Isabel, D. Using red mud bauxite for the neutralization of acid mine tailings: A column leaching test. *Can. Geotech. J.* **2006**, *43*, 1167–1179. [CrossRef]